Supporting information

Graphene Oxide Thin Film with Dual Function Integrated into a Nanosandwich Device for in Vivo Monitoring of Interleukin-6

*Meng Qi,[a] Jiawei Huang,[b] Hui Wei,[a] Chaomin Cao,[a] Shilun Feng,[c] Qing Guo,[d] Ewa M. Goldys,[c] Rui Li,[b] Guozhen Liu[a,c,e]**

[a]Key Laboratory of Pesticide and Chemical Biology of Ministry of Education, College of Chemistry, Central China Normal University, Wuhan, 430079, P. R. China

[b]Hubei Key Laboratory of Genetic Regulation and Integrative Biology, School of Life Sciences, Central China Normal University, 152 Luoyu Road, Wuhan, 430079, P. R. China

[c]ARC Centre of Excellence in Nanoscale BioPhotonics (CNBP), Macquarie University, Sydney, 2109, Australia

[d]School of Public Health, Huazhong University of Science and Technology, 13 Hangkong Road, Wuhan, 430030, P. R. China

[e]Department of Molecular Sciences, Macquarie University, Sydney, 2109, Australia

*To whom correspondence should be addressed. Email: gzliu@mail.ccnu.edu.cn

1. Modification of Gold Surface with 4-Aminphenyl

The gold electrode was first modified with 4-nitrophenyl to form Au-ph-NO_2 by scanning electrode in 0.5 M HCl solution containing 1 mM and 1 mM 4-nitroaniline for two cycles at the scan rate of 100 mV s^{-1} (Figure S1 a). The reductive peak at 0.18 V emerged in the first cycle, and disappeared in the second cycle, suggesting the successfully attachment of 4-nitrophenyl to gold surfaces. The nitro groups on Au-ph-NO_2 surfaces were converted to amine groups by scanning the Au-ph-NO_2 surface in ethanol/HCl solution (V_{H2O}/V_{EtOH} =1:9) for two cycles at the scan rate of 100 mV s^{-1} (Figure S1 b).

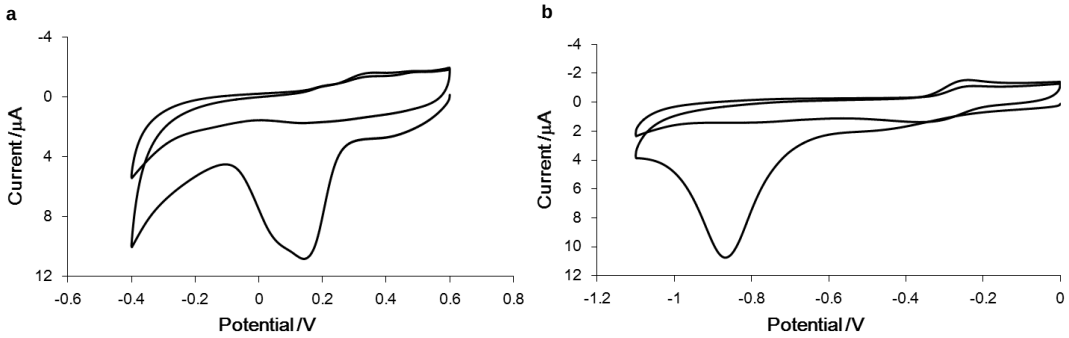

Figure S1. (a) The cyclic voltammetry of gold electrode in 0.5 M HCl solution containing 1 mM and 1 mM 4-nitroaniline at the scan rate of 100 mV s^{-1}. (b) The cyclic voltammetry of 4-nitrophenyl modified gold electrode in ethanol/HCl solution (V_{H2O}/V_{EtOH} =1:9) at the scan rate of 100 mV s^{-1}.

2. Modification of GO Surfaces with PPC

Modification of PPC to Au-ph-GO surfaces was carried out by scanning Au-ph-GO surfaces in 0.5 M HCl solution containing 1 mM and 1 mM PPC for two cycles at the scan rate of 100 mV s^{-1} (Figure S2). The reductive peak at -0.4 V emerged in the first cycle, and disappeared in the second cycle, suggesting a successful attachment of PPC molecules to gold surfaces.

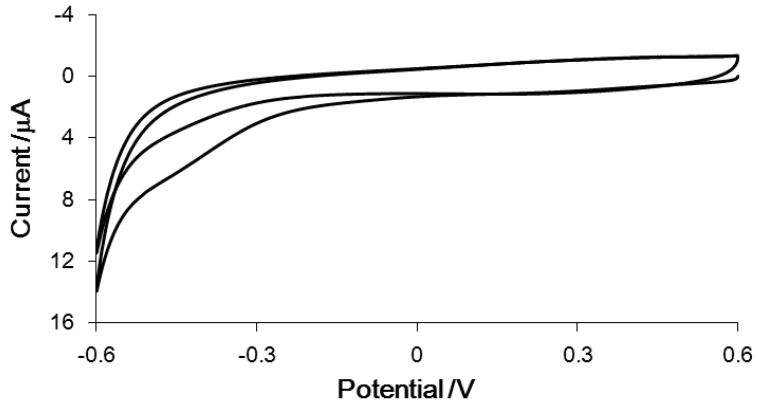

Figure S2. The cyclic voltammetry of gold electrode in 0.5 M HCl solution containing 1 mM and 1 mM PPC at the scan rate of 100 mV s^{-1}.

3. Optimization of the Attachment of NB to GO

To optimize the signal report GO-NB, the concentration of NB reacted with GO were investigated (Figure S3). With increasing of concentration of NB solution from 0.5 to 5 mM, the current intensity increased significantly, because more NB was attached on GO. Further increase concentration of NB caused the decrease of SWV intensity, which might be due to the excess NB inhibiting the reaction. Therefore, 3 mM was selected as the optimal concentration in this work.

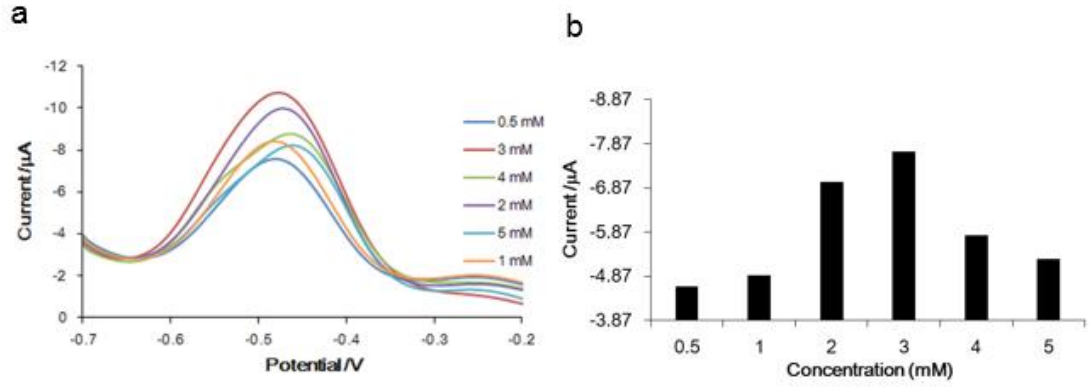

Figure S3. (a) The square wave of glassy carbon electrode in phosphate buffer solution. (b) The change in NB current with the concentration of NB added to GO solution.

4. Optimization of the Incubation Time of GO Based Nanoprobe Ab_2-GO-NB and the Effect of PPC on Resisting Non-Specific Adsorption of Ab_2-GO-NB

The incubation time of Ab_2-GO-NB has been optimized for detection of IL-6 based on

this fabricated sensing interface. It was observed that the current signal increased with the incubation time and reached a plateau when the incubation time was 30 min (Figure S4 a). Thus 30 min was chosen as the optimized incubation time. The electrochemistry of Au-ph-GO-PPC/Ab_1 surfaces and Au-ph-GO/Ab_1 surfaces in PBS solution after incubation of Ab_2-GO-NB for 30 min was recorded in Figure S4 b.

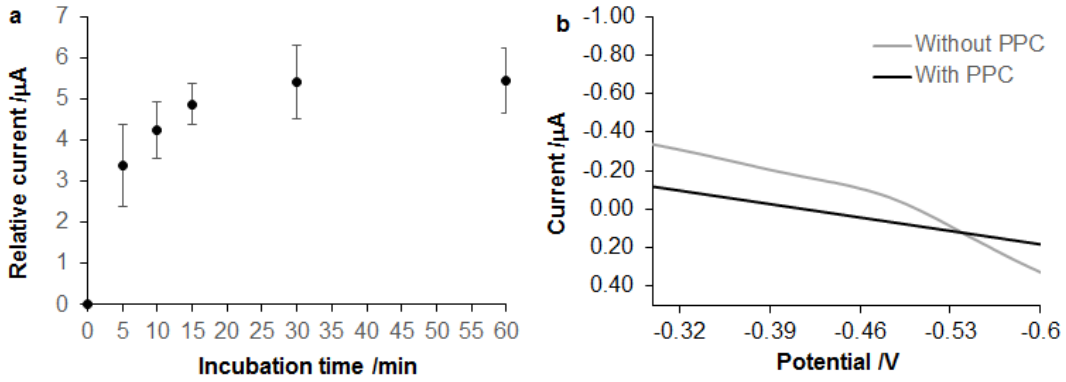

Figure S4. a) The relationship between the current and the incubation time of the fabricated nanosandwich assay in Ab_2-GO-NB. b) The square wave of the Au-ph-GO/Ab_1 surfaces and Au-ph-GO-PPC/Ab_1 surfaces in PBS buffer after incubation of Ab_2-GO-NB for 30 min.

5. Comparison of the Performance of the Thin Film GO-Based Immunosensor and General GO-Based Immunosensor for Detection of IL-6

In order to demonstrate the superior performance of the thin film of GO modified sensing interface for detection of IL-6, the general GO-based immunosensor was fabricated by dropping 5 μL of GO (0.5 mg mL^{-1}) to the bare gold electrode surface to form a layer of GO followed by modification of PPC and IL-6 capture antibodies Ab_1. The electrochemistry of the thin-film GO-based immunosensor and the general GO-based immunosensor for detection of 50 pg mL^{-1} IL-6 was compared in Figure S5. It was observed that the peak current obtained by the thin film GO-based immunosensor was about 4 times higher than that by the general GO-based immunosensor, which suggests the more efficient electrical communication was achieved by the thin film GO-based immunosensor than that by the general GO-based immunosensor.

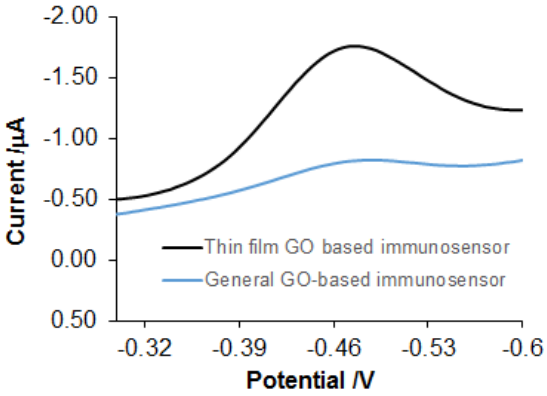

Figure S5. The square wave of thin-film GO-based immunosensor and the general GO-based immunosensor for detection of 50 pg mL^{-1} IL-6 in PBS buffer (pH7.4).

6. The Selectivity and Stability of Fabricated GO Based Nano-Sandwich Devices

To investigate the selectivity of fabricated nanosandwich assay, IL-6 was detection with the presence of five potentially interfering proteins, such as bovine serum albumin (BSA), prostate specific antigen (PSA), cancer antigen 125 (CA-125), and mouse IgG (Figure S5 a). The concentration of IL-6 and BSA is 25 pg ml^{-1} and 50 mg ml^{-1}, respectively The concentration of PSA, CA-125 and IgG is 0.5 mg ml^{-1}. The result demonstrated a good selectivity of IL-6. The stability of the immunosensor was investigated by a cyclic voltammetry scan of Au-ph-GO-PPC/Ab_1-Ag-Ab_2-GO-NB 10 cycles in PBS at a scan rate of 100 mv s^{-1}, the result show that there is no obvious change of cyclic voltammetry curve (Figure S5 b), suggesting a good stability of the sensing interfaces.

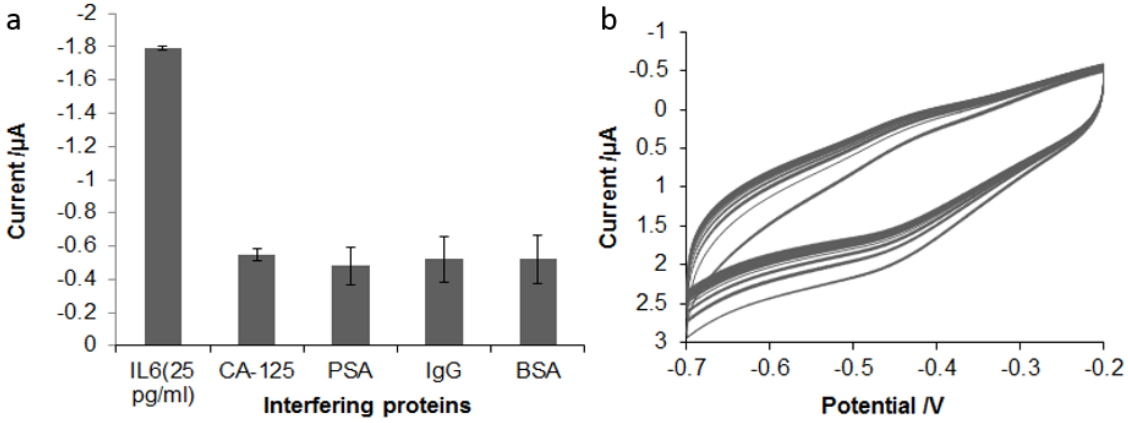

Figure S6. (a) The peak current responses of the immunosensor to 0.5 mg ml^{-1} PSA, CA-125, IgG, and 50 mg ml^{-1} BSA, as well as 25 pg ml^{-1} IL6. (b) Cyclic Voltammograms of the immunosensor scan 10 cycles.

7. **Comparison of the Performance of the Herein Fabricated Immunosensor with the Reported Biosensors for Detection of IL-6**

Table S1 shows the performance of different electrochemical biosensors for detection of IL-6 in the literature.

Table S1 Comparison of the performance of reported biosensors for detection of IL-6.

Sensors	Performance			
	Signal	Linear range (pg mL^{-1})	LOD (pg mL^{-1})	Stability
Sensor in this work	Electrochemistry	1-300	1	30 days
Li et al[1]	Electrochemistry	2–20000	1	1 month
Liu et al[2]	Fluorescence	1–400	1	9 days
Toma et al[3]	Surface plasmon enhanced fluorescence spectroscopy	2-2000	2	2 weeks
Huang et al[4]	Field effect transistor assay	4.7- 300	1.53	-
Shi et al[5]	Electrochemistry	0.01-10^6	0.1	-
Lou et al[6]	Electrochemistry	0.1-10^5	0.059	-
Chen et al[7]	Field effect transistor assay	1-100	1.37	3 months

8. *In Vivo* Animal Tests

The prepared gold wire based sensing device has been used for detection of IL-6 in mouse brain as shown in Figure S6. The performance of the sensing devices for *in vivo* detection has been evaluated using ELISA.

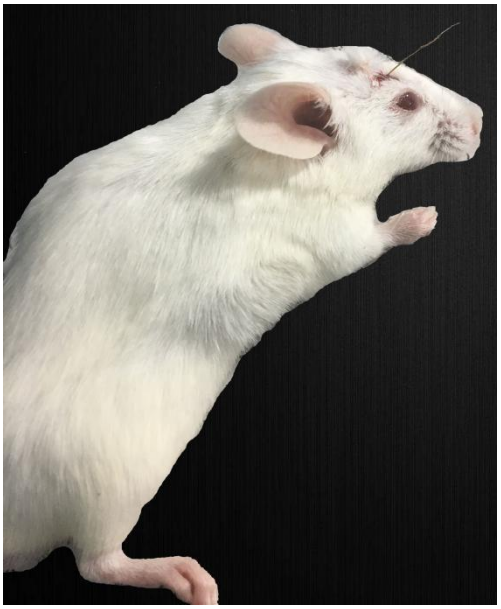

Figure S7. Image of the gold wire based nano-sandwich sensing device inserted into the mouse brain.

References

(1) Li, T.; Yang, M. Electrochemical Sensor Utilizing Ferrocene Loaded Porous Polyelectrolyte Nanoparticles as Label for the Detection of Protein Biomarker IL-6. *Sens. Actuators B Chem.* **2011,** *158* (1), 361-365.

(2) Liu, G. Z.; Qi, M.; Zhang, Y.; Cao, C. M.; Goldys, E. M. Nanocomposites of Gold Nanoparticles and Graphene Oxide Towards an Stable Label-Free Electrochemical Immunosensor for Detection of Cardiac Marker Troponin-I. *Anal. Chim. Acta* **2016,** *909*, 1-8.

(3) Toma, M.; Tawa, K. Polydopamine Thin Films as Protein Linker Layer for Sensitive Detection of Interleukin-6 by Surface Plasmon Enhanced Fluorescence Spectroscopy. *ACS Appl. Mater. Interfaces* **2016,** *8* (34), 22032-22038.

(4) Huang, J.; Chen, H.; Niu, W.; Fam, D. W.; Palaniappan, A.; Larisika, M.; Faulkner, S. H.; Nowak, C.; Nimmo, M. A.; Liedberg, B. Highly Manufacturable Graphene Oxide Biosensor for Sensitive Interleukin-6 Detection. *RSC Adv.* **2015,** *5* (49), 39245-39251.

(5) Shi, J.-J.; He, T.-T.; Jiang, F.; Abdel-Halim, E.; Zhu, J.-J. Ultrasensitive Multi-Analyte Electrochemical Immunoassay Based on GNR-Modified Heated Screen-Printed Carbon Electrodes and PS@ PDA-Metal Labels for Rapid Detection of MMP-9 and IL-6. *Biosens. Bioelectron.* **2014,** *55*, 51-56.

(6) Lou, Y.; He, T.; Jiang, F.; Shi, J.-J.; Zhu, J.-J. A Competitive Electrochemical Immunosensor for the Detection of Human Interleukin-6 Based on the Electrically Heated Carbon Electrode and Silver Nanoparticles Functionalized Labels. *Talanta* **2014,** *122*, 135-139.

(7) Chen, H.; Choo, T. K.; Huang, J.; Wang, Y.; Liu, Y.; Platt, M.; Palaniappan, A.; Liedberg, B.; Tok, A. I. Y. Label-free Electronic Detection of Interleukin-6 using Horizontally Aligned Carbon Nanotubes. *Mater. Design* **2016,** *90*, 852-857.